Research Article

Haihai Hou*, Shujun Liu, Longyi Shao*, Yonghong Li, Ming'en Zhao, and Cui Wang

Elemental geochemistry of the Middle Jurassic shales in the northern Qaidam Basin, northwestern China: Constraints for tectonics and paleoclimate

https://doi.org/10.1515/geo-2020-0318 received August 08, 2021; accepted November 08, 2021

Abstract: The elemental geochemical characteristics of mudstones/shales are good tracers for indicating the evolution of tectonics, paleoenvironment, and paleoclimate. Based on the continuous sampling of drilling cores from the Middle Jurassic Dameigou and Shimengou Formations in the northern Qaidam Basin, the major, trace, and rare earth elements of the 31 mudstones and shales were analyzed. The information on the evolution of tectonics, provenance, and paleoclimate during Middle Jurassic was also recovered. The results show that: (1) A couple of elements consisting of Sc, Y, V, Cr, Co, Ni, Cu, Zn, Th, and U are relatively enriched, indicating that the contents of siderophile and chalcophile elements are significantly high in the Middle Jurassic samples; (2) Changes in the chemical index of alteration, Ga/Rb, and K₂O/Al₂O₃ ratios in the mudstone/shale samples suggest that the paleoclimate was changed from warm and humid in the early stage to cold and dry in the middle stage and to hot and arid in the late stage; (3) The Middle Jurassic provenance of the northern Qaidam Basin was predicted from upper crust and felsic rocks to the mixed felsic rocks and basic rocks; (4) The Middle Jurassic tectonic background was changed from passive continental margin to active continental margin and oceanic island arc. The paleoclimatic and paleogeographic evolution of northern Qaidam Basin

were closely related to the surrounding paleo-oceanic and ancient plate activities. In the early stage of the Middle Jurassic, the extensional activity in the passive continental margin and the water vapor input was caused by the Tethys Ocean, resulting in a warm and humid paleoclimate. In the late stage of the Middle Jurassic, the tectonic background of the study area tended to be an oceanic island arc caused by compressive tectonic, which blocked the monsoon input and led to a hot and arid paleoclimate. The establishment of multiple geochemical profiles can provide a scientific basis for the climate changes in greenhouse–icehouses and source–sink systems of the Middle Jurassic in northwestern China.

Keywords: northern Qaidam Basin, middle Jurassic, element geochemistry, weathering, paleoclimate

1 Introduction

The Middle Jurassic shale in the northern Oaidam Basin is characterized by wide distribution, large thickness, and good preservation, which is not only an important marker for strata correlation but also an important exploration object for shale gas and oil shale [1]. In response to the current situation of shale gas exploration and development in this region, the Oil and Gas Resources Investigation Center of China Geological Survey has implemented the "Investigation of Geological Conditions for Shale Gas Formation in the Qaidam Basin" and the Chaiye-1 (CY-1) well was drilled in the Yuqia coalfield, which is the first shale gas parameter well in the northern Qaidam Basin for the Jurassic terrestrial basin. The exploration results show that three sets of gas-bearing mudstones and shales with a cumulative thickness of 141 m are found in the CY-1 well, and the thickest section is 58.12 m. In addition, the Middle Jurassic shales in the Qaidam Basin are characterized by relatively high gas content, strong

Yonghong Li: No. 105 Exploration Team, Qinghai Bureau of Coal Geological Exploration, Xining 810007, China

^{*} Corresponding author: Haihai Hou, College of Mining, Liaoning Technical University, Fuxin 123000, China, e-mail: houmensihai@163.com

^{*} Corresponding author: Longyi Shao, College of Geoscience and Surveying Engineering, China University of Mining and Technology, Beijing 100083, China, e-mail: ShaoL@cumtb.edu.cn Shujun Liu, Ming'en Zhao, Cui Wang: College of Mining, Liaoning Technical University, Fuxin 123000, China

compressibility, good pore connectivity, and abundant organic matter types [2,3]. Therefore, it is believed that the northern Qaidam Basin has a good prospect for the shale gas and oil shale development.

The elemental geochemical information of mudstones/shales have been mostly used to analyze the weathering denudation, provenance properties, and tectonic background of source areas as well as the paleoclimatic, paleogeographic, and tectonic features [4–6]. During sedimentary processes, clastic rocks primarily have undergone weathering, transportation, deposition, and diagenesis. Therefore, unstable geochemical elements are relatively deficient. whereas stable elements are considerably enriched in sedimentary rocks [7]. The elements in mudstones and shales can be classified as major elements, trace elements, and rare earth elements according to their content ratios, which are generally determined by X-ray fluorescence (XRF) and inductively coupled plasma mass spectrometry (ICP-MS), respectively. The major elements and their combinations can be divided into several guantitative parameters including chemical index of alteration (CIA), chemical index of weathering, and plagioclase alteration index. Based on the comprehensive analysis of these three parameters, previous investigations conclude that CIA is frequently used because it is less influenced by other factors to distinguish weathering index and paleoclimate in the source areas [8,9]. The variation in CIA values is usually used to analyze the degree of weathering and tectonic processes in the source areas during the sedimentary period, which can further reveal the intrinsic factors of the sedimentary process controlled by climatic and tectonic evolution [4,5]. The distribution characteristics of trace elements and rare earth elements can not only be used to study the depositional environment, provenance, and tectonic background but can also be used to recover the paleoenvironmental and tectonic evolution processes and determine the provenance properties during the depositional period [6,10,11]. Because CIA values are primarily influenced by different ranges of latitude and surface temperatures, the variation pattern in CIA values can be analyzed for the sedimentary weathering conditions and their paleoclimatic environments. The triangle diagrams and elemental distribution diagrams of CIA values are generally calculated from the various rock-source areas, which can infer the relationships between paleoclimate and sedimentary conditions [9]. Trace elements in mudstones/shales are not easily affected by water bodies and metamorphism in a series of processes including weathering, deposition, transportation, and post-diagenesis, and hence the combination of trace elements and their ratios can be used as good indicators of provenance properties and tectonic background [6,12].

Although a great resource potential is found within the Middle Jurassic strata, there is no substantial breakthrough in the exploration and development of shale gas in the northern Qaidam Basin, which would be attributed to a lack of full research on the tectonic background and paleogeographic pattern based on mudstones' and shales' elemental geochemistry. This study investigates the elemental geochemical characteristics of the Middle Jurassic mudstones/shales in the northern Qaidam Basin based on a series of XRF and ICP-MS experiments. According to the distribution of major, trace, and rare earth elements, the paleoclimatic characteristics, tectonic background, and provenance properties in the northern Qaidam Basin were analyzed. This study not only provides a theoretical basis for tectonic evolution and gas exploration of the Jurassic basins but also furnishes a scientific basis for analyzing the climate change in greenhouse-icehouses and the source-sink systems in the northern Qaidam Basin.

2 Geological settings

The Qaidam Basin is situated in the northeastern Tibetan Plateau and is one of the three major inland basins in China. This basin is rich in coal, oil, gas, potassium, and graphite resources, and has a great exploration potential in those resources. The northern Qaidam Basin is rich in unconventional natural gas resources of the Jurassic coal measures, and is a strategic replacement area for coalbed methane and shale gas exploration and development [13]. The northern Qaidam Basin is surrounded by the Altun Mountains to the west and the Qilian Mountains to the north, accompanied with the Saishiteng Mountain, Lyuliang Mountain, Xitie Mountain, Olongbuluke Mountain, Aimunke Mountain, and Maoniu Mountain from west to east (Figure 1).

The samples of this study came from the YQ-1 drilling cores, and this well was drilled in the Yuqia coalfield of the northern Qaidam Basin for the Jurassic shale gas exploration (Figure 2). The depositional systems including alluvial fan delta-lacustrine facies are primarily developed during the Middle Jurassic period in the northern Qaidam Basin [2,14]. Specifically, the Dameigou Formation, lower Shimengou Formation, and upper Shimengou Formation are dominated by the deltaic plain, shore-shallow lake, and deep-semideep lake, respectively (Figure 2). In terms of lithology distribution, the Dameigou Formation is dominated by non-marine coarse-grained to fine-grained silicious clastic rocks, with thick coal seams interbedded in the lowest section, whereas the Shimengou Formation

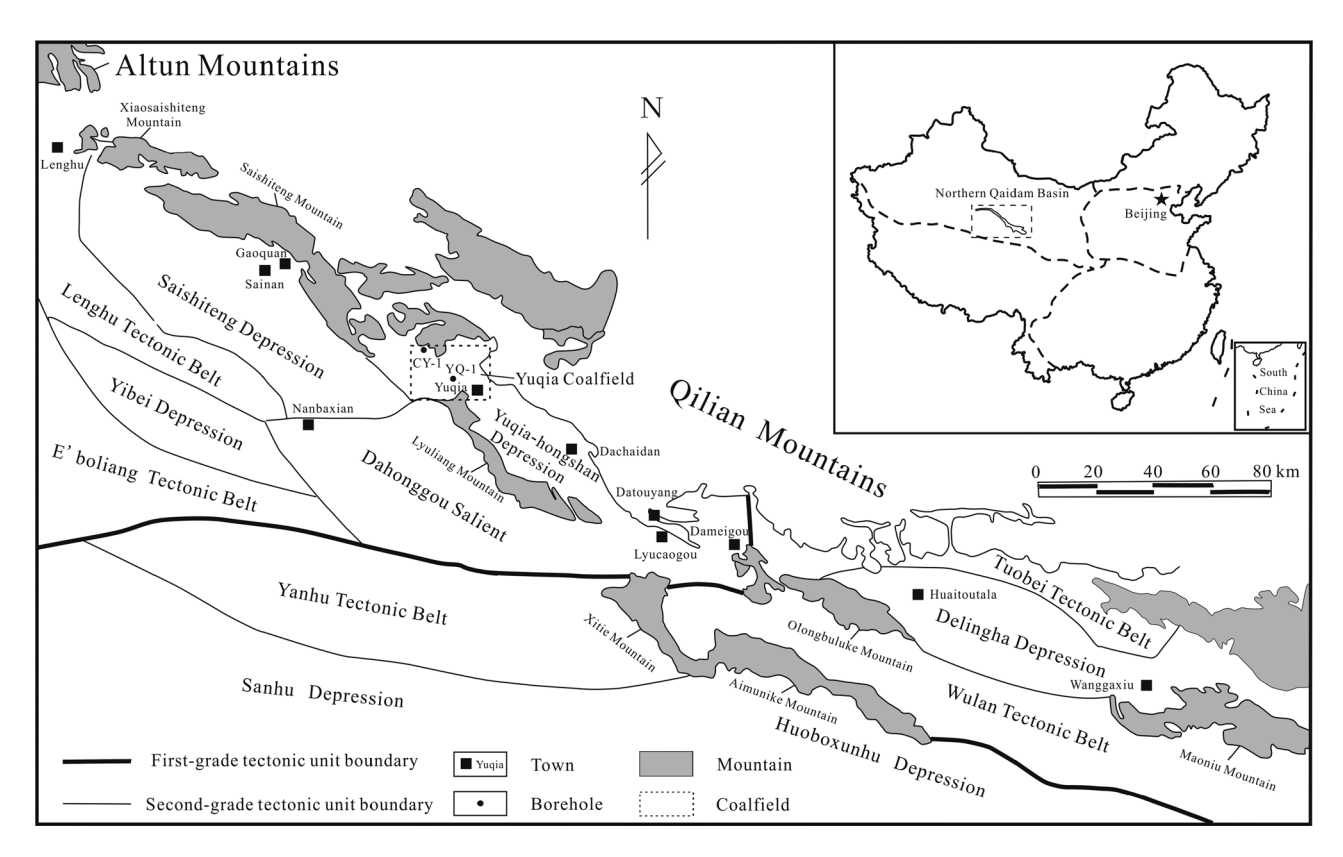


Figure 1: Tectonic outline and distribution of sampling sites in the northern Qaidam Basin.

consists of gray-white medium and coarse sandstones in the lower section and brown thick lacustrine shales in the upper section (Figure 2). It should be noted that a section of brown oil shale is stably distributed at the top of the upper Shimengou Formation, which can be used as a marker for the regional strata correlation in the northern Qaidam Basin [1]. A large-scale migration of the Middle Jurassic sedimentary centers from west to east and from south to north is found in the northern Qaidam Basin, forming the Yuqia and Dameigou sedimentary centers [15], with overlying thinning to the Lyucao Mountain, Lyuliang Mountain, and Aimunike Mountain. The rock sources come from the basement uplift on the north and south sides and the Altun Mountains on the northwest side [2,14].

3 Samples and methodology

3.1 Sample collection

As the elemental geochemical distribution in the mudstones and shales are more stable and advantageous for analyzing sources identification and paleoclimatical recovery [16,17], a total of 31 mudstone/shale samples

have been taken from the YQ-1 well in the northern Qaidam Basin in this study. Specifically, 14 samples were collected from the upper Shimengou Formation, 10 samples from the lower Shimengou Formation, and 7 samples from the Dameigou Formation (Figure 2). After the macroscopic description in field, the collected samples were wrapped with preservative film prior to laboratory tests and analyses.

3.2 Experimental methods

3.2.1 Element geochemistry tests

The major elements including SiO₂, Al₂O₃, Fe₂O₃, MgO, CaO, Na₂O, K₂O, MnO, TiO₂, and P₂O₅ were tested by an XRF spectrometer at Beijing Research Institute of Uranium Geology. The shale powders and lithium metaborate flux were mixed in a ratio of 1:10 and fused at 1,050°C in a Pt–Au crucible. Then, the cooled mixed melt was put on a glass disk for XRF analysis. According to the Chinese National Standard GB/T 14506.30-2010, the alkaline fusion glass sheet method was used for testing the trace and rare earth elements of the mudstones and shales. Each sample

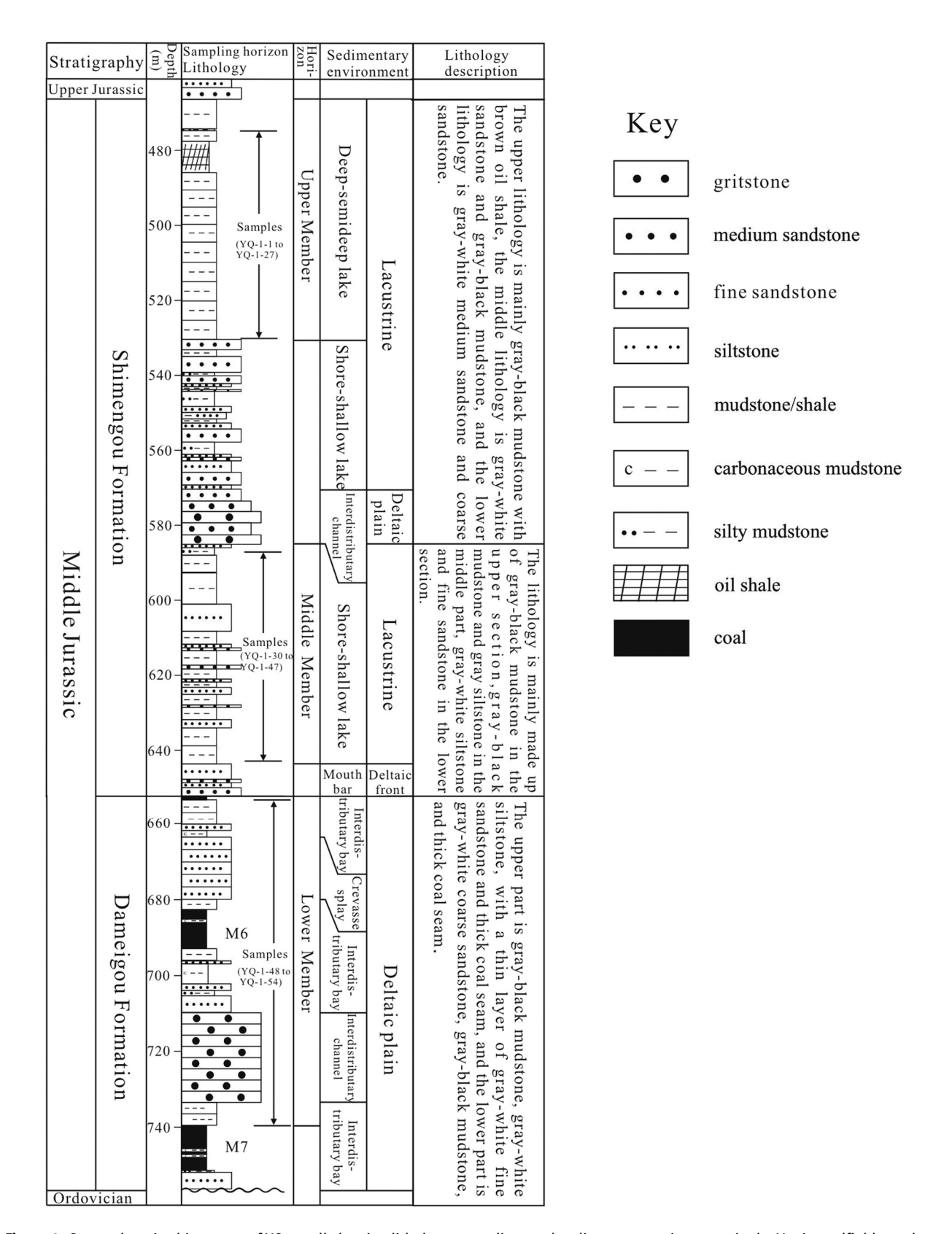


Figure 2: Comprehensive histogram of YQ-1 well showing lithology, sampling, and sedimentary environment in the Yuqia coalfield, northern Qaidam Basin (14 samples from upper Shimengou Formation: YQ-1-1 to YQ-1-27; 10 samples from lower Shimengou Formation: YQ-1-30 to YQ-1-47; 7 samples from Dameigou Formation: YQ-1-48 to YQ-1-54).

was placed in a high temperature furnace, and relevant organic matters were removed with analysis errors lower than 1% after adding a series of chemical reagents. The ICP-MS was used to determine the trace and rare earth elements of the samples, and the particle size of each sample should be crushed to lower than 74 µm. The 25 mg sample was weighed and sealed in the container with the weight accuracy of 0.01 mg. Then, 1 mL of HF and 0.5 mL of HNO₃ were added, of which 50 mg liquids were heated to 185 ± 5 °C within 24 h. After cooling and evaporating until nearly dry with adding 0.5 mL of HNO₃, it was then heated at 130°C for 3 h for ICP-MS testing. The testing process mainly included the standard mixed solution adjustment, calibration data collection, blank solution analysis, and interference coefficient measurement.

3.2.2 CIA

The chemical weathering corresponds to the decrease in feldspars in rocks (kalium, sodium, and calcium elements) and the increase in clay minerals (iron and aluminum elements). The greater the CIA value, the stronger the chemical weathering of the sediments [18-22]. The CIA value can be calculated as follows: CIA = molar $(Al_2O_3/[Al_2O_3 + Na_2O + CaO^* + K_2O]) \times 100$, where mole number in each oxide is necessary, and CaO* refers to CaO in silicate minerals. As carbonate and phosphate minerals also contain CaO, an indirect method to calculate CaO^* was proposed by Mclennan [23]. $CaO^* = molar$ $(CaO-P_2O_5 \times 10/3)$ when Na₂O content is higher than that of CaO*; otherwise, CaO* = molar Na₂O. The sample with higher CIA value likely means that the weathering process is losing a large amount of Ca, Na, and K compared to the stable Al and Ti, revealing a warm and humid paleoclimate. In addition, the lower CIA value reflects a cold and dry climatic condition in the regions [24]. Generally, the weathering degree can be divided into weak, moderate, and strong stages, corresponding to CIA values with 50-60%, 60-80%, and 80-100%, respectively [24].

4 Results

4.1 Major element characteristics

The major element results of the Middle Jurassic mudstones and shales in the northern Qaidam Basin are shown in Table 1. Generally, the SiO₂ content of all the samples is the highest, followed by Al₂O₃ and Fe₂O₃,

whereas the K₂O, MgO, CaO, TiO₂, Na₂O, P₂O₅, and MnO contents are relatively low (Table 1 and Figure 3). Specifically, the SiO₂, Al₂O₃, and Fe₂O₃ contents in the upper Shimengou shales range from 19.27 to 53.64% (average 42.67%), 6.14 to 23.03% (average 17.22%), and 2.79 to 18.36% (average 8.76%), respectively. In terms of the lower Shimengou shales, the SiO₂, Al₂O₃, and Fe₂O₃ contents range from 47.92 to 68.19% (average 59.74%), 16.97 to 26.13% (average 23.10%), and 1.38 to 5.45% (average 2.07%), respectively. The SiO₂, Al₂O₃, and Fe₂O₃ contents of the Dameigou shales range from 46.46 to 60.34% (average 56.29%), 20.87 to 26.92% (average 24.09%), and 1.01 to 4.32% (average 2.08%), respectively. Thus, the upper Shimengou shales have the lowest SiO₂ and Al_2O_3 contents, with the highest Fe_2O_3 content (Table 1; Figure 3). In addition, the SiO₂ and Al₂O₃ contents and CIA values first decrease and then increase from the Dameigou Formation to the upper Shimengou Formation, with the minimum value appearing at the top of the upper Shimengou Formation (Figure 3). The Na₂O content first increases and then decreases from the bottom to the top with the maximum value appearing in the middle of the upper Shimengou Formation. The Fe₂O₃, MgO, CaO, MnO, and P₂O₅ contents are relatively low in the Dameigou Formation and the lower Shimengou Formation, whereas a relatively high value appears in the upper Shimengou Formation. The contents of K₂O and TiO₂ are higher in the Dameigou Formation and lower Shimengou Formation than those in the upper Shimengou Formation (Figure 3). Therefore, there are great variations in the major elements in the Middle Jurassic shales, which indicate that the paleoclimate and paleoenvironment also should be significantly changed in these strata in the northern Oaidam Basin.

4.2 Trace element characteristics

Each trace element and their combinations can be good indicators for determining provenance properties [12,25]. In order to analyze the enrichment characteristics of trace elements of the Middle Jurassic mudstones and shales in the northern Qaidam Basin, the distributions of most trace elements and their implications are shown aided by the standard cobweb drawings (Figure 4). The variations in the trace elements in the northern Qaidam Basin are basically similar between the Damengou and Shimengou shales. However, it should be noted that the elements consisting of Sc, Y, V, Cr, Co, Ni, Cu, Zn, and Ba are relatively enriched in the Dameigou Formation,

Table 1: Major element compositions and CIA values of the Middle Jurassic mudstones/shales in the Yuqia coalfield, northern Qaidam Basin

Unit	Sample	Lithology	SiO ₂	Al ₂ 0 ₃	Fe ₂ 0 ₃	MgO	Ca0	Na ₂ O	K ₂ 0	MnO	Ti0 ₂	P ₂ 0 ₅	101	CIA (%)
	number		(wt%)	(wt%)	(wt%)	(wt%)	(wt%)	(wt%)	(wt%)	(wt%)	(wt%)	(wt%)	(wt%)	
Upper Shimengou	YQ-1-1	Gray-black mudstone	31.20	14.17	7.68	2.96	14.52	0.26	1.42	0.159	0.484	0.169	26.44	85.50
Formation	YQ-1-3	Brown oil shale	42.83	17.82	7.88	3.11	4.76	0.37	1.83	0.140	0.568	0.150	20.06	84.79
	YQ-1-5	Brown oil shale	19.27	6.14	2.91	4.82	25.27	0.30	0.82	0.153	0.250	0.377	39.67	76.61
	YQ-1-7	Brown oil shale	30.61	6.42	2.79	1.85	26.63	98.0	0.91	0.162	0.255	0.263	29.74	74.67
	YQ-1-9	Gray-black mudstone	49.00	17.09	10.77	1.71	0.73	0.51	2.22	0.630	0.635	0.176	16.46	92.08
	YQ-1-11	Gray-black mudstone	51.77	17.39	6.87	1.81	0.75	0.58	2.24	0.404	0.636	0.208	17.35	80.37
	YQ-1-13	Gray-black mudstone	53.49	18.74	5.22	1.88	0.48	0.58	2.43	0.131	0.672	0.092	16.25	81.55
	YQ-1-15	Gray-black mudstone	53.64	20.33	5.49	1.91	0.40	0.49	2.71	0.122	0.749	0.122	13.98	82.94
	YQ-1-17	Gray-black mudstone	47.50	19.96	10.22	1.55	69.0	0.37	2.12	0.524	0.711	0.406	15.89	86.20
	YQ-1-18	Gray-black mudstone	36.77	15.79	18.36	1.83	2.73	0.30	1.77	0.940	0.569	1.630	19.29	84.52
	YQ-1-20	Gray-black mudstone	49.65	22.36	7.34	1.66	0.44	0.33	2.24	0.286	0.761	0.175	14.72	86.98
	YQ-1-22	Gray-black mudstone	45.65	21.11	11.67	1.39	0.65	0.23	2.29	0.363	0.725	0.194	15.65	86.71
	YQ-1-24	Gray-black mudstone	46.32	23.03	9.48	1.22	0.88	0.23	2.22	0.271	0.797	0.486	14.97	87.92
	YQ-1-27	Gray-black mudstone	39.63	20.67	15.93	1.03	1.00	0.19	1.94	0.269	099.0	0.215	18.42	88.34
Lower Shimengou	YQ-1-30	Gray-black mudstone	58.53	25.19	2.14	0.75	0.19	0.16	2.50	0.014	1.040	0.045	9.36	88.71
Formation	YQ-1-32	Gray-black mudstone	47.92	26.13	1.71	08.0	0.23	0.20	2.45	0.008	0.786	0.086	19.67	89.05
	YQ-1-33	Carbonaceous	58.64	25.16	1.91	0.85	0.17	0.19	2.82	0.010	0.950	0.051	9.12	87.62
		mudstone												
	YQ-1-34	Carbonaceous	68.19	16.97	1.92	0.44	0.15	0.16	2.34	0.005	976.0	0.036	8.72	85.04
		mudstone												
	YQ-1-35	Gray-black mudstone	57.69	23.67	1.57	0.73	0.20	0.19	2.96	0.007	0.836	0.064	11.98	86.35
	YQ-1-36	Carbonaceous	62.33	23.22	1.40	0.61	0.15	0.19	2.75	0.007	0.947	0.056	8.21	87.13
		mudstone												
	YQ-1-39	Gray-black mudstone	61.55	23.46	1.39	0.70	0.15	0.18	2.84	900'0	1.010	0.056	8.5	96.98
	YQ-1-41	Gray-black mudstone	60.14	23.82	1.79	0.57	0.16	0.15	2.63	0.016	0.961	0.070	9.54	88.07
	YQ-1-44	Gray-black mudstone	61.52	18.96	5.45	1.25	0.43	0.16	2.58	0.039	968.0	0.000	8.51	85.06
	YQ-1-47	Gray-black mudstone	60.87	24.45	1.38	0.64	0.13	0.18	2.80	0.008	0.931	0.040	8.48	87.55
Dameigou	YQ-1-48	Carbonaceous	46.46	26.90	1.57	0.64	0.19	0.20	2.52	0.007	0.799	0.072	20.62	89.26
Formation		mudstone												
	YQ-1-49	Carbonaceous	58.64	22.27	4.32	09.0	0.24	0.14	2.55	0.093	0.936	0.115	10.07	87.55
		mudstone												
	YQ-1-50	Dark grey mudstone	53.81	20.87	4.21	0.48	0.15	0.14	2.19	0.033	0.832	0.073	17.15	88.53
	YQ-1-51	Carbonaceous	56.99	26.92	1.24	0.59	0.16	0.15	2.28	9000	0.894	990.0	10.66	90.44
		mudstone												
	YQ-1-52	Carbonaceous	57.92	26.19	1.17	0.56	0.14	0.14	2.22	9000	0.886	0.041	10.62	90.33
		mudstone	;	;	;		:	;	;				!	;
	YQ-1-53	Dark grey mudstone	59.90	22.54	1.01	0.57	0.12	0.14	2.63	0.004	0.952	0.103	12	88.05
	TQ-1-54	Dark grey mudstone	00.34	16:77	1.00	0.55	0.11	0.15	7.30	0.000	0.934	0.100	11.14	00.51

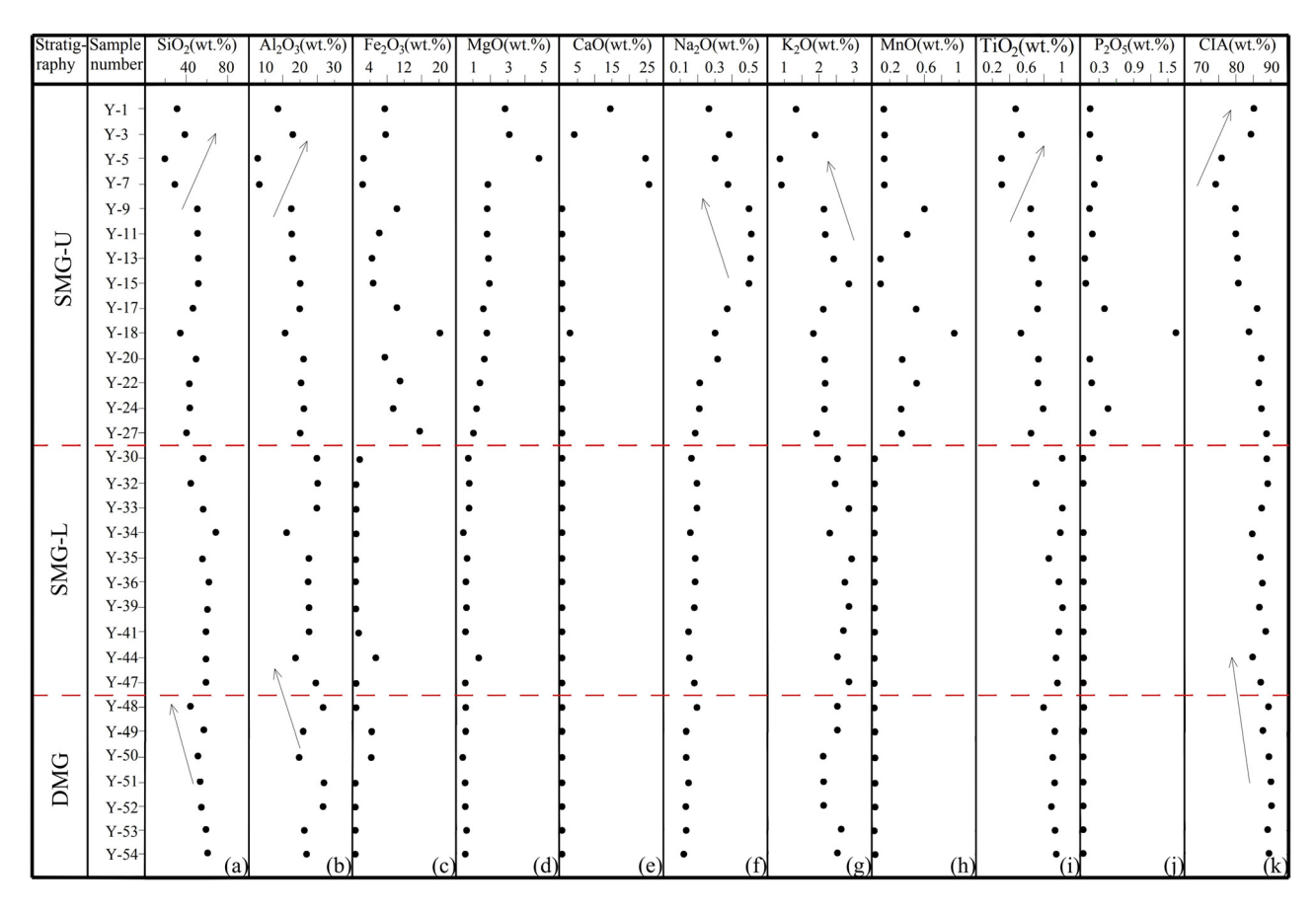


Figure 3: The vertical distribution of major elements of the Middle Jurassic shales in the drilling YQ-1 well, Yuqia coalfield, northern Qaidam Basin (SMG-U: upper Shimengou Formation; SMG-L: lower Shimengou Formation; DMG: Dameigou Formation. (a) SiO₂; (b) Al₂O₃; (c) Fe₂O₃; (d) MgO; (e) CaO; (f) Na₂O; (g) K₂O; (h) MnO; (i) TiO₂; (j) P₂O₅; (k) CIA).

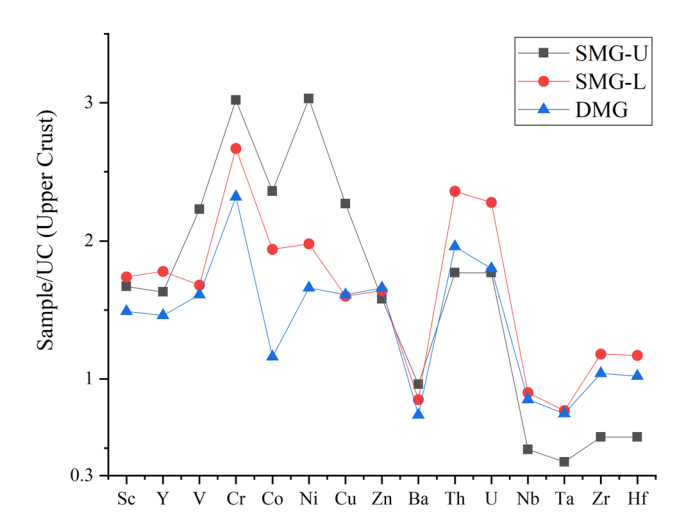


Figure 4: Standardized cobweb diagram of trace elements in the Dameigou and Shimengou shales (UC, upper crust-normalized value of each trace element).

whereas other elements including Th, U, Nb, Ta, Zr, and Hf are relatively deficient in the Dameigou Formation (Table 2). Compared with the average trace element contents in the upper crust, several elements including Sc, Y, V, Cr, Co, Ni, Cu, Zn, Th, and U are relatively enriched, while Zn, Nb, Ta, Zr, and Hf elements are relatively deficient in the Middle Jurassic strata. These indicate that siderophile and chalcophile elements were significantly enriched in the study area during the Middle Jurassic period, while lithophile elements were relatively deficient.

4.3 Rare earth element characteristics

Rare earth elements mainly existed in detrital grains, which are more stable during the sedimentary process of mudstones/shales. They are not easily influenced by external factors, and can effectively reflect the provenance characteristics in the study area [26,27]. Therefore, it is possible to use rare earth elements to quantitatively analyze the physical properties of the sediments [28] and the changes in paleoclimate during the sedimentary period [29]. The rare earth elements of the Middle Jurassic

Table 2: Trace element compositions of the Middle Jurassic mudstones and shales from the Yuqia coalfield, northern Qaidam Basin

Unit	Sample	Sc	>	בי	Be	>	ڻ	೦	Ξ	n C	Zn	Ga F	Rb S	Sr	Cs B	Ва Т	Ę	_	g Q	Та	Zr	Ŧ
Upper	Y-1	11.9	27.1	30.2	1.75	76	58.3	16.6	56.6	55.2	58.4	16.5 7	79.1 4	454 5	5.29 4	492 1	12.9 4	4.12	8.3	0.659	78.8	2.44
Formation	Y-5	7.2	17.2	13	0.822	80.5	57.1	11.3	28.7	41.7			_					5.74	4.55	0.322	42.1	1.27
	γ-7	9.32	21.1	12.6	1.19	72	58	11.9	37.3	29.6						-		1.85	96.4	0.369	42.7	1.32
	γ-9	19.6	38.9	45.9	3.94	129	126	32.7	98.5	57.4								4.3	13.7	1.01	116	3.5
	Y-11	19.6	39.2	45.6	3.34	147	109	20.2	63.4	61.2								4.41	13.5	0.941	109	3.42
	Y-13	21.7	40.7	51.1	3.1	134	119	28.1	75.5	89								5.74	14.5	1.03	124	3.66
	Y-15	22.1	43.7	49.5	3.68	165	128	26.7	84.4	62								5.92	14.4	1.01	129	4.01
	Y-17	23.2	39.5	49.3	3.63	168	140	29.3	70.2	6.79								2.48	13.8	0.983	118	3.63
	γ-18	17.7	37.8	41.6	3.1	163	104	21.5	48.2	44.1								4.17	12.1	0.849	99.2	3.06
	Y-20	25	42.7	26.7	3.33	178	147	33.5	6.62	73								7.11	15.1	1.04	132	4.2
	Y-22	24.2	44	55.2	3.98	135	131	30.2	59.5	53.7								5.41	15.8	1.18	154	4.69
	Y-24	24.1	44.7	60.1	3.48	145	108	27.1	53.7	45.3								5.21	16.4	1.22	153	4.69
	Y-27	24.3	38.5	52.5	3.57	161	113	23.7	45.9	53.1								4.84	13.5	1.01	133	4.11
Lower	Y-30	18.2	33.2	57.4	3.28	79.4	98.2	21.4	9.74	33.6			_					2.97	25.3	1.89	196	5.95
Shimengou	Y-32	27.6	59.6	71.4	4.47	183	145	8.39	31.4	75.3								9.33	18.3	1.43	200	5.93
Formation	γ-33	21.1	40.5	8.89	2.89	118	95.7	17.3	20	35.6						_		5.27	22.4	1.61	195	60.9
	Y-34	17.5	28.6	37.7	2.37	77.9	9.9/	32.3	36.4	26.7								4.84	25.2	1.81	345	10.1
	γ-35	15.9	46.8	55.4	3.85	8.76	102	18.8	37.7	45.6								7.11	18.6	1.52	218	6.81
	Y-36	19.4	40	58.3	2.85	93.9	103	30.2	55.8	46.5								8.14	24.4	1.81	238	7.26
	Y-39	21.8	41.8	57.8	3.65	88.1	97.2	67.6	27.7	37.8				_				5.85	25.7	1.83	247	7.31
	Y-41	16.2	44.2	48.7	3.69	93	74.1	32	48.3	40.5								7.79	25.3	2	243	7.12
	Y-44	15.5	28.4	36.6	2.7	72	6.99	18.9	34.9	28.1								4.63	18.2	1.44	177	5.32
	Y-47	17.7	27.9	52	2.69	107	75.8	2.7	25.3	29.5			_					4.89	21.9	1.68	183	5.75
Dameigou	Y-48	17.7	34.8	55.8	5.53	75.1	82	13.3	39.3	38.7								5.23	17.9	1.3	173	5.45
Formation	٧-49	15	38.1	45.2	2.73	88.5	81.3	11	21.1	36.2								5.18	22.8	1.65	229	29.9
	Y-50	13.6	33.5	38.8	2.45	92.2	72.8	14.8	43.5	27.1								5.42	18.8	1.48	217	90.9
	Y-51	15.5	25.1	64.7	2.89	105	71.8	12	35.7	48								4.19	24.7	2.05	186	5.68
	Y-52	14.6	22.8	65.3	1.92	78.2	8.99	5.4	20.4	31.1								3.76	18.9	1.52	155	4.79
	Y-53	20.3	37.3	45.9	4.1	124	104	19.2	48.5	42.6								6.11	23.4	1.79	223	95.9
	Y-54	17.9	32.8	45.6	3.45	113	2.66	2.7	23.5	97.6								5.38	21.4	1.69	194	6.04

Sample number YQ-1-1 is abbreviated as Y-1; The units of these trace elements are µg/g.

Table 3: Rare earth compositions of the Middle Jurassic mudstones and shales from the Yuqia coalfield, northern Qaidam Basin

Unit	Sample number	Га	e G	P.	PN	Sm	п	P9	₽	Dy	웊	占	Ē	ХÞ	ŋ	ΣREE	ΣLREE	ΣHREE	ΣLREE/ ΣHREE	La/Yb
Upper	γ-1	37.1	26	8.04	30.1	6.05	1.19	5.01	0.88	4.95	0.95	2.73		2.83	0.39	159.66	141.48	18.18	7.78	13.11
Shimengou	γ-3	40.2	62.4	8.93	34.3	6.34	1.31	5.51	0.93	5.11	96.0	2.71		2.8	0.4	172.34	153.48	18.86	8.14	14.36
Formation	γ-5	19.9	41.1	4.69	18.1	3.65	0.75	3.21	0.54	2.97	0.59	1.66		1.67	0.22	99.3	88.19	11.11	7.94	11.92
	۲-۲	24.7	46.5	5.44	20.8	4.01	98.0	3.77	0.63	3.46	69.0	1.95		2.06	0.29	115.47	102.31	13.16	7.77	11.99
	٧-9	55.4	92.7	11.6	44.1	8.33	1.74	7.41	1.24	6.75	1.31	3.82		4.02	0.57	239.6	213.87	25.73	8.31	13.78
	Y-11	50.3	87.6	11	43.8	8.44	1.7	7.25	1.26	6.44	1.28	3.6		3.88	0.57	227.72	202.84	24.88	8.15	12.96
	Y-13	62.9	110	13.4	53.5	6.67	1.95	8.43	1.41	7.57	1.39	3.91		4.39	0.61	280.06	251.72	28.33	8.89	14.33
	Y-15	63.1	119	14.1	53.1	9.93	1.92	8.78	1.47	7.8	1.48	4.11	0.71	4.47	99.0	290.63	261.15	29.48	8.86	14.12
	Y-17	61.1	119	14.5	54.9	10.4	2.12	8.78	1.41	7.53	1.44	4.09		4.16	9.0	290.68	262.02	28.66	9.14	14.69
	Y-18	47.1	84.6	10.7	41.2	7.96	1.53	6.9	1.19	6.2	1.23	3.44		3.65	0.54	216.82	193.09	23.73	8.14	12.90
	Y-20	74.6	136	17	65.8	11.9	2.45	10.1	1.56	8.42	1.45	4.24		4.51	0.62	339.34	307.75	31.59	9.74	16.54
	Y-22	64.4	120	14.8	57.3	10.4	1.96	8.71	1.48	7.94	1.52	4.33		4.49	0.67	298.71	268.86	29.85	9.01	14.34
	Y-24	66.5	130	15.4	58.8	11.3	2.17	8.6	1.58	8.46	1.54	4.39		4.53	0.64	315.82	284.17	31.65	8.98	14.68
	Y-27	29	107	13	51.7	9.35	1.85	8.01	1.32	7.06	1.35	4.02		4.29	0.63	269.22	241.9	27.32	8.85	13.75
Lower	Y-30	57.9	101	12.4	46.8	8.37	1.38	7.34	1.2	6.38	1.16	3.37		3.62	0.52	251.98	227.85	24.13	9.44	15.99
Shimengon	Y-32	99.4	184	21.5	83.8	14.2	2.65	12.1	2.07	10.3	1.96	5.75		5.83	0.89	445.36	405.55	39.81	10.19	17.05
Formation	Y-33	57.7	102	11.9	45.8	8.12	1.5	6.94	1.23	6.75	1.3	3.72		4	0.57	252.15	227.02	25.13	9.03	14.43
	Y-34	39.4	71.1	8.44	31.7	5.81	98.0	4.75	98.0	69.4	96.0	2.94		3.44	0.53	175.98	157.31	18.66	8.43	11.45
	Y-35	79.8	163	19	75.4	14	2.39	11.2	1.85	6	1.58	4.45		4.27	0.65	387.25	353.59	33.66	10.50	18.69
	Y-36	9.09	121	14.3	54.1	89.6	1.69	∞	1.45	7.54	1.36	3.88		4.06	0.56	288.83	261.37	27.46	9.52	14.93
	γ-39	58.4	106	12.9	49.7	8.77	1.68	8.06	1.34	7.39	1.39	3.98		4.5	0.68	265.45	237.45	28	8.48	12.98
	Y-41	66.5	126	15.5	59.5	10.6	1.88	8.5	1.45	7.53	1.47	4.18		4.21	0.63	308.6	279.98	28.63	87.6	15.80
	Y-44	42.7	78	9.21	34.7	6.15	1.14	5.11	0.92	4.89	0.95	2.85		3.1	0.43	190.63	171.9	18.73	9.18	13.77
	Y-47	47.1	79.5	9.93	37	6.31	1.14	5.29	0.95	4.82	96.0	2.8		3.01	0.43	199.72	180.98	18.73	99.6	15.65
Dameigou	Y-48	61.8	111	14.4	52.5	9.82	1.78	∞	1.38	6.95	1.28	3.62		3.71	0.55	280.37	254.3	26.07	9.75	16.66
Formation	Y-49	57.1	109	11.8	45.7	8.37	1.41	6.45	1.19	6.32	1.25	3.58		3.84	0.55	257.17	233.38	23.79	9.81	14.87
	Y-50	51	104	11.6	6.44	7.91	1.39	6.32	1.15	5.88	1.13	3.31		3.39	0.48	243	220.8	22.2	9.95	15.04
	Y-51	49.8	77.3	10	36.5	5.84	96.0	4.82	0.87	4.7	6.0	2.67		2.73	0.42	197.95	180.4	17.55	10.28	18.24
	Y-52	37.5	57.5	7.33	56	4.35	92.0	3.88	0.73	3.8	0.79	2.2		2.45	0.35	148.01	133.44	14.58	9.15	15.31
	Y-53	59.2	118	13.6	54.6	10.1	1.79	8.22	1.43	7.01	1.34	3.75		3.95	0.55	284.18	257.29	26.89	9.57	14.99
	Y-54	51.9	100	11.9	45.2	8.29	1.51	6.97	1.22	6.25	1.13	3.32		3.46	0.5	242.19	218.8	23.39	9.35	15.00

Sample number YQ-1-1 is abbreviated as Y-1; The units of these rare earth elements are $\mu g/g$.

shales in the northern Qaidam Basin are shown in Table 3. The average values of Σ REE, Σ LREE, Σ HREE, and Σ LREE/ ΣHREE in the Dameigou, lower Shimengou, and upper Shimengou shales are 236.12, 214.06, 22.07 μ g/g, and 9.69; 276.60, 250.30, 26.29 µg/g, and 9.42; and 236.81, 212.35, 24.47 µg/g, and 8.55, respectively, indicating that the light rare earth elements are enriched and the heavy rare earth elements are deficient in the Middle Jurassic shales in the northern Qaidam Basin. The average values of La/Yb in the upper Shimengou, lower Shimengou, and Dameigou shales are 13.82, 15.07, and 15.73, respectively, suggesting that the accumulation ability of light rare earth elements in the upper Shimengou shales are lower than the lower Shimengou and Dameigou shales (Table 3). This enrichment of light rare earth and the deficiency of heavy rare earth are also found compared to the average rare earth element in the upper crust [30] (Figure 5). The La element is the most enriched among the light rare earth elements, while the Gd element is the most enriched among the heavy rare earth elements.

5 Discussion

5.1 Chemical weathering and its implication for paleoclimate

The average CIA value of the Middle Jurassic shales in northern Qaidam Basin is 89.26% with 88.95% in the Dameigou Formation, 87.15% in the lower Shimengou

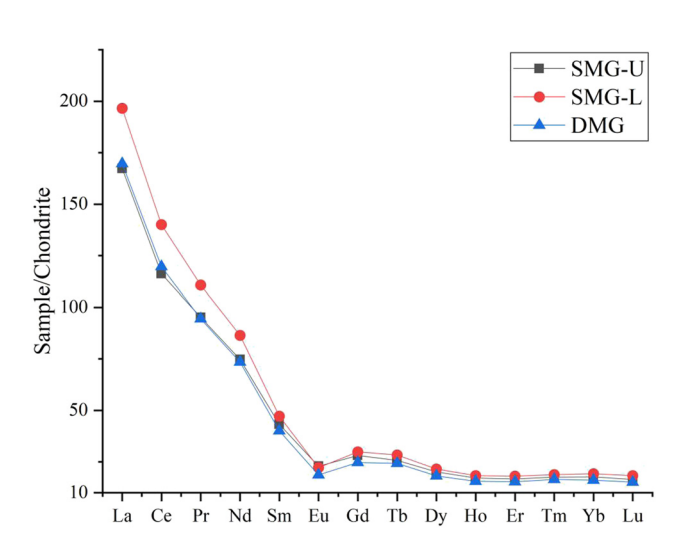


Figure 5: Standardized cobweb diagram of rare earth elements in the Middle Jurassic shales (Chondrite, chondrite-normalized value of each rare earth element).

Formation, and 85.65% in the upper Shimengou Formation. The maximum value of CIA occurs in the Dameigou Formation with a value of 90.44%, and the minimum value of CIA is found in the upper Shimengou Formation with a value of 74.67% (Table 1 and Figure 6). These indicate that the weathering degree of the Middle Jurassic shales in the northern Qaidam Basin is relatively high and the chemical weathering degree from the Dameigou Formation to the upper part of the Shimengou Formation has a decreasing trend during the deposition process (Figure 6). The different combinations of Al, K, Rb, and Ga elements in the shales can also be used to analyze the chemical weathering intensity and the characteristics of paleoclimatical changes in the sedimentary period [31]. The Al and Ga elements are mainly associated with the composition of fine-grained aluminosilicate and are enriched in kaolinite minerals representing warm and humid climate [32]. The K and Rb elements are closely related to illite, with higher values representing a weaker chemical weathering intensity under an arid, wet, and cold climate [32]. Therefore, illite-rich sediments should have low Ga/Rb and high K₂O/Al₂O₃ ratios, while kaolinite-rich sediments have high Ga/Rb and low K2O/Al2O3 ratios [31]. In this study, the Ga/Rb ratios in the mudstones/shales generally decrease from the Dameigou Formation to the upper part of the Shimengou Formation, whereas the K₂O/Al₂O₃ ratios show an opposite trend (Figure 7), revealing a gradual shift from a warm and humid to a cold and dry paleoclimatic condition during

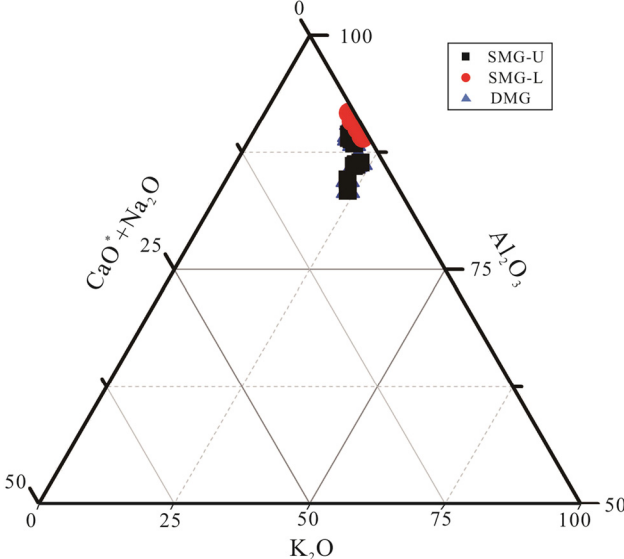


Figure 6: $Al_2O_3 - CaO^* + Na_2O - K_2O(A - CN - K)$ ternary diagram showing the changes in chemical compositions and weathering degree in the Dameigou and Shimengou shales.

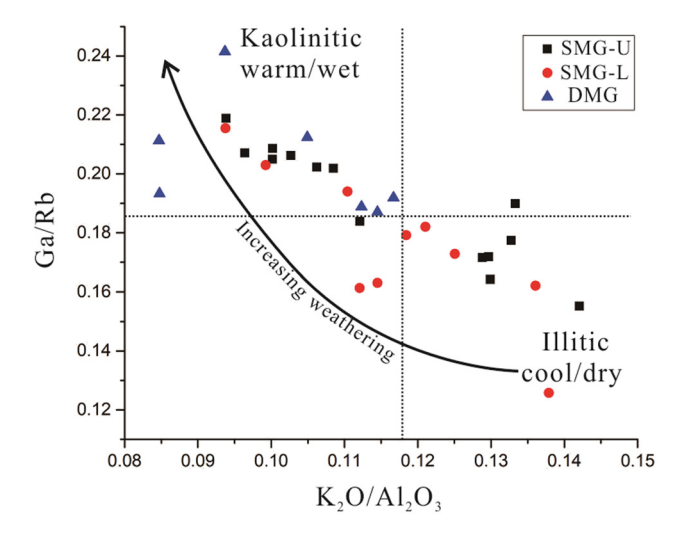


Figure 7: Chemical weathering intensity and paleoclimate evolution of the Middle Jurassic shales in the Yuqia coalfield, northern Qaidam Basin (Ga/Rb vs. K_2O/Al_2O_3). The samples from Dameigou Formation are restricted in the range of Ga/Rb higher than 0.187 and K_2O/Al_2O_3 lower than 0.1167.

the Middle Jurassic. It is worth noting that the Ga/Rb and K_2O/Al_2O_3 ratios in the lower and upper Shimengou Formation shales belong to a mostly fluctuating trend, not an abrupt change (Figure 7). Combined with previous studies [4,33], the paleoclimate was changed from warm and humid to cold and dry in the early Middle Jurassic and then it changed into hot and arid in the late Middle Jurassic. In this study, there is a coal seam with thickness higher than 8 m in the Dameigou Formation, but it changes into

a thin layer and directly disappears in the upper Shimengou Formation (Figure 2). Meanwhile, the lithology of the Upper Jurassic is mostly covered with red sand conglomerates [33–35], which also confirms that the depositional period was shifted from a warm and humid in the early stage to a cold and dry in the middle stage and then to a hot and arid paleoclimate in the late stage.

5.2 Provenance analyses

The sedimentary provenance is generally analyzed using several indicators consisting of framework petrography, heavy minerals, and element geochemistry [36-38]. The source rock types of sedimentary rocks can be largely determined using the La/Yb-\(\sum_REE\) diagram in shales [39]. Most samples in the study area are distributed in the mixed area between granite and alkaline basalt, with a few samples falling in the intersection area of sedimentary rock and alkaline basalt (Figure 8a). Therefore, it is considered that the provenance of the Middle Jurassic strata in the study area was mainly from alkaline basalts and granites, with a few from sedimentary rocks. Based on the relationship between La/Th and Hf [40], the distributions of the shale samples in the study area are relatively concentrated, indicating that the parent rock types tended to be consistent. The provenances were mainly from felsic rocks and mixed sources of felsic rocks and basic rocks, with a few from the upper crust (Figure 8b).

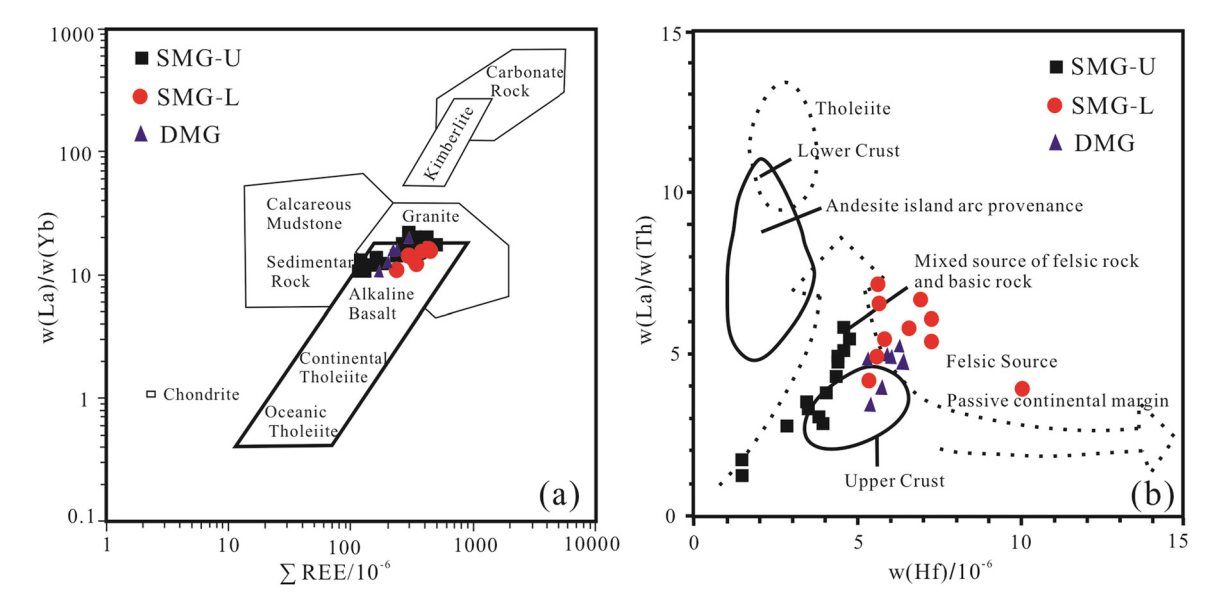


Figure 8: Discrimination diagrams for provenance attribute of the Middle Jurassic shales in the Yuqia coalfield, northern Qaidam Basin (a) with the base map after Allègre and Minster [39], (b) with the base map after Floyd and Leveridge [40].

Specifically, a vertical change rule of the source rocks from bottom to top can also be found, with the upper crust and felsic sources in the Dameigou Formation, felsic sources in the lower Shimengou Formation, and with the mixed sources of felsic rocks and basic rocks in the upper Shimengou Formation (Figure 8b). This indicates that a great change would be effected for the tectonic background in the northern Qaidam Basin.

5.3 Tectonic background discrimination

Based on the discriminant diagram of SiO₂-K₂O/Na₂O proposed by Roser and Korsch [41], most of the samples fall in the region of passive continental margin except for a few samples which belong to the active continental margin and the oceanic/continental island arc peripheral regions in the upper Shimengou Formation (Figure 9a). This indicates that the tectonic background of the source rocks in the Middle Jurassic Dameigou and Shimengou formations is mostly characterized by passive continental margin. A few samples fall in the active continental margin and oceanic/continental island arc area, which are mainly attributed to low SiO₂ contents, probably caused by weathering [20]. In addition, based on the distribution characteristics of each sample point, the tectonic background generally changed from the passive continental margin of the Dameigou Formation to the active continental margin and the oceanic island arc of the Upper Shimengou Formation (Figure 9a). According to the La–Th–Sc trace element discriminative tectonic background illustration proposed by Bhatia [42], the samples from the Middle Jurassic strata of YQ-1 well in the Yuqia coalfield are shown in the La–Th–Sc triangle map. The results show that the samples from the upper Shimengou Formation fall in the continental island arc region, and the Dameigou shales fall in the active and the passive continental margin regions (Figure 9b). It should be noted that the lower Shimengou shales are found in both these regions. Therefore, the tectonic settings of the Middle Jurassic Dameigou Formation in the study area were mostly characterized by passive or active continental margin, but the Shimengou period showed a tendency shifting to the continental island arc region.

5.4 Indication for the tectonic, climatic, and depositional system

There are several various rules for the tectonics, paleoenvironmental, and paleoclimatic evolution from the Middle Jurassic Dameigou Formation to Shimengou Formation in the northern Qaidam Basin. These changes were generally characterized by a shift in the tectonic setting from the passive continental margin to the active continental margin and oceanic island arc; a shift in rock sources from the upper crust and felsic rocks to the mixed felsic rocks and basic rocks; and a shift in paleoclimate from warm and humid

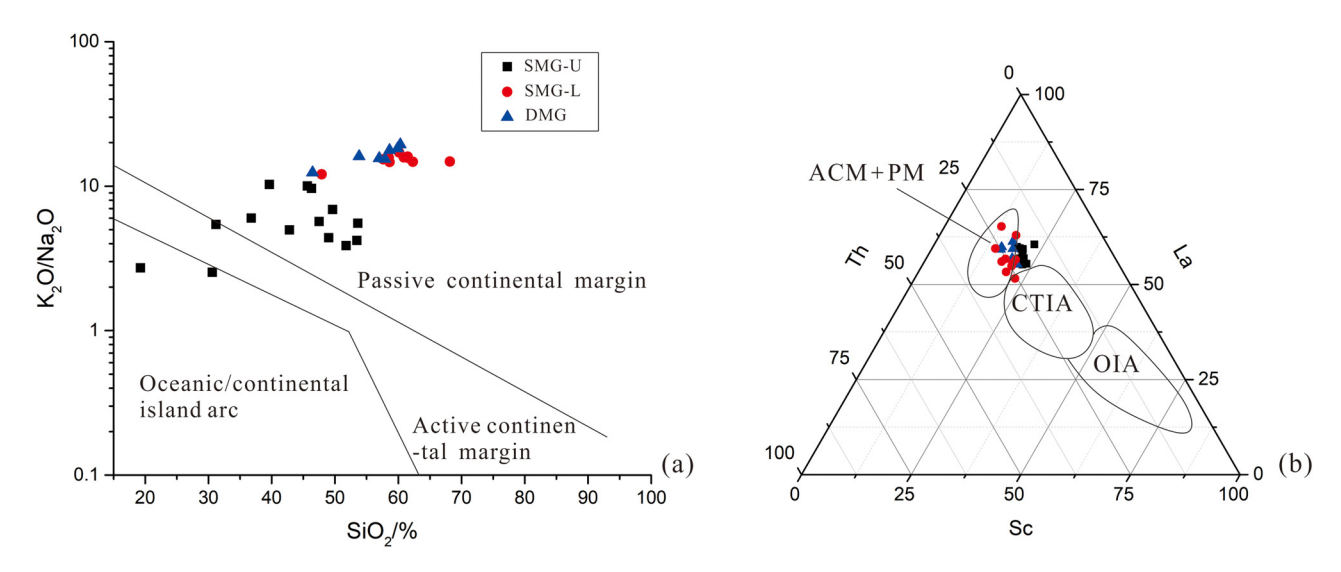


Figure 9: Discrimination diagrams for tectonic setting of the Middle Jurassic shales in the Yuqia coalfield, northern Qaidam Basin (a) with the base map after Roser et al. [41], (b) with the base map after Bhatia [42]; A-SiO₂-K₂O/Na₂O; B-La-Th-Sc; CTIA: continental island arc; OIA: oceanic island arc; ACM: active continental margin; PM: passive continental margin.

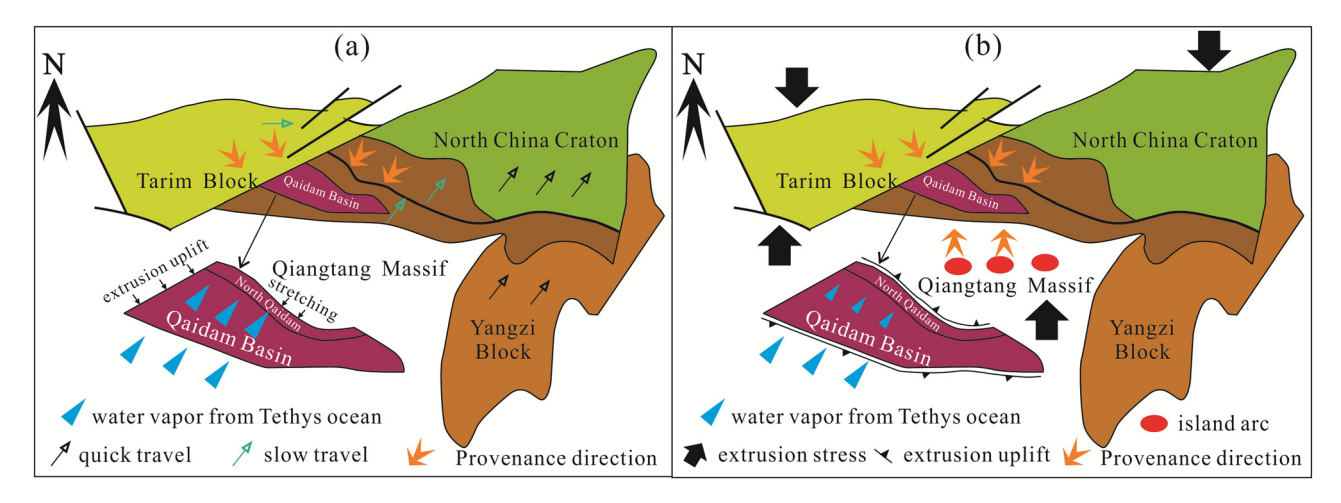


Figure 10: Model showing the evolution for tectonic, climatic, and depositional system from early to late Middle Jurassic in the northern Qaidam Basin. (a) Early Middle Jurassic and (b) Late Middle Jurassic.

to cold and dry and then to hot and arid. The relevant sedimentary facies were shifted from peatlands in the deltaic floodplain to mudstones in shallow lakes and oil shales in semi-deep lakes [1,2]. During the Jurassic, the Qaidam Basin was surrounded by the Tethys Ocean, Qiangtang Massif, Tarim Block, North China Craton, and Yangzi Block (Figure 10). Thus, the paleoclimatic and paleogeographic evolution of the Qaidam Basin were closely related to these paleo-oceanic and ancient plate activities [43,44]. In the early Middle Jurassic, the different movements of the Qiangtang Massif and the North China Craton resulted in a tectonic extensional environment in the northern Qaidam Basin [43]. This tectonic background corresponded to a passive continental margin, and the provenance directions mainly came from the northern and western parts of northern Qaidam Basin [2], which mainly provided upper crust and felsic rocks as the source rock types (Figures 8 and 10). At the same time, the overall topography of the Qaidam Basin was low, and the water vapor from the Tethys Ocean led the study region to be wet and rainy [33], which provided favorable conditions for the formation of thick coal seams under these warm and humid climates. Therefore, the abundant coal and coalbed methane resources were found in the Middle Jurassic Dameigou Formation [45,46]. In the late Middle Jurassic, a remarkable lift caused by the extrusion and collision of the Tarim Block in the west and the Qiangtang Massif in the south, blocked the transport of the Tethys Ocean monsoon [33] and the temperature of the region greatly increased under the influence of the dry climate zone and the strengthening global greenhouse effect [47], which resulted in a hot and arid climate stage. The Shimengou shales and oil shales were well deposited in the prevailed lacustrine paleoenvironments under these paleoclimates [48]. Plate extrusion and collision simultaneously causing the development of island arc and the upwelling of basic and ultrabasic iron with magnesium-rich magma, finally resulted in the oceanic island arc in tectonic background as well as the mixed felsic rocks and basic rocks in rock sources during the late Middle Jurassic (Figures 8 and 10).

6 Conclusion

- (1) Based on the analyses of elemental geochemistry and the lithological changes, the paleoclimate of the Middle Jurassic in the northern Qaidam Basin was shifted from warm and humid in the early stage to cold and dry in the middle stage and then to hot and arid in the late stage.
- (2) The vertical changes in trace and rare earth elements in the samples suggest that the Middle Jurassic tectonic background of the northern Qaidam Basin was changed from passive continental margin to active continental margin and oceanic island arc, and the corresponding rock sources were changed from the upper crust and felsic rocks to the mixed felsic rocks and basic rocks.
- (3) Due to the passive continental margin of tectonic background during the early Middle Jurassic, there was a warm and humid paleoclimate caused by the extensional tectonics and the water vapor input from the Tethys Ocean. The late Middle Jurassic extrusion resulted in the development of island arc and blocked the monsoon input, making the tectonic background

- of this period tending to be oceanic island arc with a hot and arid paleoclimate.
- (4) Since elemental geochemistry can only provide qualitative study results, it is difficult to vertically determine the degree of paleoclimatical dryness, wetness, and cooling. Therefore, it is suggested that more quantitative geochemical parameters such as carbon, oxygen isotopes, and organic carbon isotopes can be used in later studies to deeply investigate the tectonic-climatic responses to the sediment changes.

Acknowledgments: We are grateful to Professor Huan Li and other anonymous reviewers for their careful comments to improve our article.

Funding information: This research work was supported by the China Postdoctoral Science Foundation (2021M693844), the Discipline Innovation Team of Liaoning Technical University (LNTU20TD-05; LNTU20TD-14; LNTU20TD-30), the Guiding Program of Liaoning Natural Science Funds (2019-ZD-0046), and the Scientific Research Funding Project of Liaoning Education Department (LJ2019JL004).

Conflict of interest: Authors state no conflict of interest.

References

- Hou HH, Shao LY, Li YH, Lu J, Li Z, Wang S, et al. Geochemistry, reservoir characterization and hydrocarbon generation potential of lacustrine shales: A case of YQ-1 well in the Yuqia Coalfield, northern Qaidam Basin, NW China. Mar Pet Geol. 2017;88:458-71.
- Li M, Shao LY, Liu L, Lu J, Spiro B, Wen HJ, et al. Lacustrine basin evolution and coal accumulation of the Middle Jurassic in the Saishiteng coalfield, northern Qaidam Basin, China. J Palaeogeography. 2016;5(3):205-20.
- Guo TX, Zhou Z, Ren SM. Jurassic shale gas discovered at Chaiye-1 well on the northern margin of Qaidam Basin. Geol China. 2017;44(2):401-2.
- Cao J, Wu M, Chen Y, Hu K, Bian LZ, Wang LG, et al. Trace and rare earth element geochemistry of Jurassic mudstones in the northern Qaidam Basin, northwest China. Geochemistry. 2012;72(3):245-52.
- Yang J, Cawood P, Du YS, Feng B, Yan JX. Global continental weathering trends across the Early Permian glacial to postglacial transition: Correlating high- and low-paleolatitude sedimentary records. Geology. 2014;42(10):835-8.
- Han SB, Zhang JC, Wang CS, Tang X, Chen ZQ. Elemental geochemistry of lower Silurian Longmaxi shale in southeast Sichuan Basin, South China: constraints for Paleoenvironment. Geol J. 2017;53(4):1458-64.

- Tanaka K, Akagawa F, Yamamoto K, Tani Y, Kawabe I, Kawai T. Rare earth element geochemistry of lake Baikal sediment: its implication for geochemical response to climate change during the last glacial/interglacial transition. Quater Sci Rev. 2007;26(9-10):1362-8.
- Panahi A, Young GM, Rainbird RH. Behavior of major and trace elements (including REE) during Paleoproterozoic pedogenesis and diagenetic alteration of an Archean granite near Ville Marie, Québec, Canada. Geochim Et Cosmochim Acta. 2000;64(13):2199-220.
- [9] Xu XT, Shao LY. Limiting factors in utilization of chemical index of alteration to quantify the degree of weathering in provenance. J Palaeogeograp. 2018;20(3):515-22.
- [10] Peng YY, Kang ZH, Li WQ, Han HY, Tan L. Element geochemical characteristics of carboniferous shale in Wuwei basin and its significance. Geoscience. 2017;30(3):574-86.
- Qu XR, Li J, Sun CR, Zhang QH, Tang SH, Wei JG. Geochemistry characteristics of rare earth elements in the late Paleozoic black shale from eastern Ordos Basin. J China Coal Soc. 2018;43(4):1084-93.
- Bhatia MR. Rare earth element geochemistry of Australian [12] Paleozoic graywackes and mudrocks: Provenance and tectonic control. Sediment Geol. 1985;45:97-133.
- [13] Shao LY, Hou HH, Tang Y, Lu J, Qiu HJ, Wang XT, et al. Selection of strategic replacement areas for CBM exploration and development in China. Nat Gas Ind B. 2015;2(2-3):211-21.
- [14] Li M, Shao LY, Lu J, Spiro B, Wen HJ, Li YH. Sequence stratigraphy and paleogeographic of the Middle Jurassic coal measures in the Yuqia coalfield, northern Qaidam Basin, northwestern China. AAPG Bull. 2014;98(12):2531-50.
- [15] Lu J, Shao LY, Liu TJ, Wen HJ, Wang H, Shang LJ, et al. A sequence stratigraphic analysis of the Jurassic coal measures in Yuqia region of Northern Qaidam basin. Coal Geol Exploration. 2007;35(1):1-6.
- Cullers RL. The controls on the major- and trace-element evolution of shales, siltstones and sandstones of Ordovician to tertiary age in the Wet Mountain region, Colorado, U.S.A. Chem Geol. 1995;123(1):107-31.
- Cullers RL. The geochemistry of shales, siltstones and sandstones of Pennsylvanian-Permian age, Colorado, USA: Implications for provenance and metamorphic studies. Lithos. 2000;51(3):181-203.
- [18] Nesbitt HW, Young GM. Prediction of some weathering trends of plutonic and volcanic rocks based on thermodynamic and kinetic considerations. Geochim Et Cosmochim Acta. 1984;48(7):1523-34.
- Franchi F, Kelepile T, Capua AD, De Wit MCJ, Kemiso O, [19] Lasarwe R, et al. Lithostratigraphy, sedimentary petrography and geochemistry of the Upper Karoo Supergroup in the Central Kalahari Karoo Sub-Basin, Botswana. J Afr Earth Sci. 2021;173:104025.
- [20] Ali S, Phartiyal B, Taloor A, Arif M, Singh BP. Provenance properties, weathering, and paleoclimatic records of the Pliocene-Pleistocene sequences of the Himalayan foreland basin, NW Himalaya. Arab J Geosci. 2021;14(3):1-14.
- Jian X, Guan P, Zhang W, Feng F. Geochemistry of Mesozoic and Cenozoic sediments in the northern Qaidam basin, northeastern Tibetan Plateau: Implications for provenance and weathering. Chem Geol. 2013;360-361:74-88.

- [22] Jian X, Zhang W, Liang HH, Guan P, Fu L. Mineralogy, petrography and geochemistry of an early Eocene weathering profile on basement granodiorite of Qaidam basin, northern Tibet: Tectonic and paleoclimatic implications. Catena. 2019;172:54-64.
- [23] Mclennan SM. Weathering and global Denudation. J Geol. 1993;101(2):295-303.
- [24] Fedo CM, Wayne Nesbitt H, Young GM. Unraveling the effects of potassium metasomatism in sedimentary rocks and paleosols, with implications for paleoweathering conditions and provenance. Geology. 1995;23(10):921-4.
- [25] Adamu CI, Omang BO, Oyetade OP, Johnson O, Nganje TN. Trace and rare earth element geochemistry of the black and grey shales of the Calabar flank, Southeastern Nigeria: constraints on the depositional environment and the degree of metal enrichment. Acta Geochim. 2020;40:312-24.
- [26] Murray RW, Buchholtz Ten Brink MR, Jones LD, Gerlach DC, Price Russ IIIG. Rare earth elements as indicators of different marine depositional environments in chert and shale. Geology. 1990;18(3):268-71.
- [27] Zhu DC, Liao ZL, Pan GT, Duan LP. Some suggestions of how to correctly use the tectonic discrimination diagrams and geochemical data. Geol-Geochem. 2001;29(3):152-7.
- [28] Cai GQ, Guo F, Liu XT, Sui SL, Li CW, Gao XF, et al. Geochemical characteristics of Neogene sedimentary rocks from Zhanhua Sag and its implication for Provenance. Geol Sci Technol Inf. 2007:26(6):17-24.
- [29] Zhou HY, Wang Q, Zhao JX, Zheng LN, Guan HZ, Feng YX, et al. Rare earth elements and yttrium in a stalagmite from Central China and potential paleoclimatic implications. Palaeogeograph Palaeoclimatol Palaeoecol. 2008;270(1-2):128-38.
- [30] Taylor SR, Mclennan SM. The continental crust: its composition and evolution. Oxford: Blackwell Scientific Publications: 1985.
- [31] Roy DK, Roser BP. Climatic control on the composition of Carboniferous-Permian Gondwana sediments, Khalaspir basin, Bangladesh. Gondwana Res. 2013;23:1163-71.
- [32] Ratcliffe KT, Wright AM, Montgomery P, Palfrey A, Vonk A, Vermeulen J, et al. Application of chemostratigraphy to the Mungaroo formation, the Gorgon Field, offshore Northwest Australia. Aus Pet Prod Explor Assoc J. 2010;50:371-88.
- [33] Hu JJ, Ma YS, Wang ZX, Liu YQ, Gao WL, Qian T. Palaeoenvironment and palaeoclimate of the middle to late Jurassic revealed by geochemical records in northern margin of Qaidam Basin. J Palaeogeography. 2017;19(3):480-90.
- [34] Hou HH, Liang GD, Shao LY, Tang Y, Mu GY. Coalbed methane enrichment model of low-rank coals in multi-coals superimposed regions: a case study in the middle section of southern Junggar Basin. Front Earth Sci. 2021;15(2):256-71.
- [35] Hou HH, Shao LY, Tang Y, Li YN, Liang GD, Xin YL, et al. Coal seam correlation in terrestrial basins by sequence stratigraphy

- and its implications for palaeoclimate and palaeoenvironment evolution. J Earth Sci. 2022;33:1-24.
- [36] Jian X, Guan P, Zhang DW, Feng F, Liu RJ, Lin SD. Provenance of Tertiary sandstone in the northern Qaidam basin, northeastern Tibetan Plateau: Integration of framework petrography, heavy mineral analysis and mineral chemistry. Sediment Geol. 2013;290:109-25.
- [37] Jian X, Guan P, Zhang W, Liang HH, Feng F, Fu L. Late cretaceous to early eocene deformation in the northern Tibetan Plateau: detrital apatite fission track evidence from northern Qaidam basin. Gondwana Res. 2018;60:94-104.
- [38] Hong D, Jian X, Fu L, Zhang W. Garnet trace element geochemistry as a sediment provenance indicator: An example from the Qaidam basin, northern Tibet. Mar Pet Geol. 2020;116:104316.
- [39] Allègre CJ, Minster JF. Quantitative models of trace element behavior in magmatic processes. Earth Planet Sci Lett. 1978;38(1):1-25.
- [40] Floyd PA, Leveridge BE. Tectonic environment of the Devonian Gramscatho basin, south Cornwall: framework mode and geochemical evidence from turbiditic sandstones. J Geol Soc. 1987;144:531-42.
- [41] Roser BP, Korsch RJ. Determination of tectonic setting of sandstone-mudstone suites using SiO₂ content and K₂O/Na₂O ratio. J Geol. 1986;94(5):635-50.
- [42] Bhatia MR. Plate tectonics and geochemical composition of sandstones: a reply. J Geol. 1983;91:611-27.
- [43] Jin JQ, Zhao WZ, Xue LQ, Meng QR. Proto-types and evolution of Jurassic Basins in NW China. Geol Rev. 1999;45(1):92-104.
- [44] Liu BQ, Shao LY, Wang XT, Li YN, Xu J. Application of channelbelt scaling relationship to Middle Jurassic source-to-sink system in the Saishiteng area of the northern Qaidam Basin, NW China. J Palaeogeography. 2019;8(2):181-97.
- [45] Lu J, Zhou K, Yang MF, Shao LY. Jurassic continental coal accumulation linked to changes in palaeoclimate and tectonics in a fault-depression superimposed basin, Qaidam Basin, NW China. Geol J. 2020;55:7998-8016.
- [46] Hou HH, Shao LY, Li YH, Li Z, Wang S, Zhang WL, et al. Influence of coal petrology on methane adsorption capacity of the Middle Jurassic coal in the Yuqia Coalfield, northern Qaidam Basin, China. J Pet Sci Eng. 2017;149:218-27.
- [47] Lu J, Zhou K, Yang MF, Eley Y, Shao LY, Hilton J. Terrestrial organic carbon isotopic composition (δ^{13} Corg) and environmental perturbations linked to Early Jurassic volcanism: evidence from the Qinghai-Tibet Plateau of China. Glob Planet Change. 2020;195:103331.
- [48] Hou HH, Shao LY, Li YH, Liu L, Liang GD, Zhang WL, et al. Effect of paleoclimate and paleoenvironment on organic matter accumulation in lacustrine shale: Constraints from lithofacies and element geochemistry in the northern Qaidam Basin, NW China. J Pet Sci Eng. 2022;208:109350.